Conformation of Bacteriochlorophyll Molecules in Photosynthetic Proteins from Purple Bacteria†

Karine Lapouge,‡ Arne Näveke,‡ Andrew Gall,‡ Anabella Ivancich,‡,§ Jérôme Seguin,‡ Hugo Scheer,|| James N. Sturgis,‡,⊥ Tony A. Mattioli,‡,▽ and Bruno Robert*,‡

Section de Biophysique des Protéines et des Membranes, Département de Biologie Cellulaire et Moléculaire/CEA et URA CNRS 2096, Centre d'Etudes Saclay, 91191 Gif/Yvette Cedex, France, and Botanisches Institut der Universität München, 80638 München, Germany

Received March 29, 1999; Revised Manuscript Received June 7, 1999

ABSTRACT: Fourier transform near-infrared resonance Raman spectroscopy can be used to obtain information on the bacteriochlorophyll *a* (BChl *a*) molecules responsible for the redmost absorption band in photosynthetic complexes from purple bacteria. This technique is able to distinguish distortions of the bacteriochlorin macrocycle as small as 0.02 Å, and a systematic analysis of those vibrational modes sensitive to BChl *a* macrocycle conformational changes was recently published [Näveke et al. (1997) *J. Raman Spectrosc. 28*, 599−604]. The conformation of the two BChl *a* molecules constituting the primary electron donor in bacterial reaction centers, and of the 850 and 880 nm-absorbing BChl *a* molecules in the light-harvesting LH2 and LH1 proteins, has been investigated using this technique. From this study it can be concluded that both BChl *a* molecules of the primary electron donor in the photochemical reaction center are in a conformation close to the relaxed conformation observed for pentacoordinate BChl *a* in diethyl ether. In contrast, the BChl *a* molecules responsible for the long-wavelength absorption transition in both LH1 and LH2 antenna complexes are considerably distorted, and furthermore there are noticeable differences between the conformations of the BChl molecules bound to the α- and β-apoproteins. The molecular conformations of the pigments are very similar in all the antenna complexes investigated.

In purple photosynthetic bacteria, the initial capture of solar photons and the subsequent transduction of the excitation energy into electrochemical potential energy occurs in light-harvesting (LH)[1] antenna proteins and reaction centers (RC), respectively. Many purple bacteria are able to synthesize two functionally distinct types of antenna, termed LH1 and LH2. The LH1 antenna is in contact with, and transfers excitation energy directly to, the RC. Indeed the two proteins can be isolated together as a RC/LH1 core complex. In contrast, the LH2 antenna generally transfers energy to LH1 and not directly to the RC. The RC uses the excitation energy to generate electrochemical potential energy, by reducing a quinone molecule on the cytoplasmic side of the membrane and oxidizing a cytochrome at the periplasmic surface. All three types of photosynthetic proteins bind bacteriochlorophyll (BChl) and carotenoid molecules as cofactors. In the LH proteins, BChl molecules absorb the incoming photons and direct the excitation energy toward the RC. In the RC, BChl molecules trigger the primary step of the transduction of excitation energy into potential chemical energy, as a dimer of excitonically coupled BChls constitute the primary electron donor (P) and a monomeric BChl the primary acceptor.

The physicochemical properties of the BChls of the RC and antenna complexes are precisely tuned by their environment, mainly including the protein host, to enable them to perform specific functions. While isolated monomeric BChl molecules absorb near 770 nm in most solvents, those bound to the LH complexes and the RC exhibit absorption maxima between 800 and 890 nm; i.e., they are red-shifted relative to the isolated pigment by as much as 1750 cm^{-1}. Equally, the oxidation potential of isolated BChl *a* is +650 mV, while in purple bacterial RCs the oxidation potential of dimer P is +500 mV (*1*−*5*), and in green bacteria it is +250 mV (*6*, *7*). Our understanding of structure/function relationships in these proteins thus requires information on the mechanisms underlying the tuning of the absorption and redox properties of the BChl cofactors.

Many different molecular mechanisms have been proposed to account for modulation of BChl absorption and redox potential properties. The underlying BChl−BChl or BChl−protein interactions involve the electrostatic properties of the BChl binding sites, π−π interactions, hydrogen bonding, and specific BChl conformations imposed by steric hindrance in the BChl binding pocket. The role of BChl−BChl and BChl−protein interactions in controlling the absorption

† This work was supported by grants from the DAAD (A.N.) and the DFG (H.S.) and a fellowship from the Royal Society (A.G.).

* Corresponding author.

‡ Section de Biophysique des Protéines et des Membranes, C. E. Saclay.

§ Present address: Section de Bioénergétique, DBCM/CEA et URA CNRS 2096, C.E. Saclay, 91191 Gif/Yvette Cedex, France.

|| Botanisches Institut der Universität München.

⊥ Present address: Laboratoire d'Ingénierie des Systèmes Macromoléculaires, UPR 9027 CNRS, 31 Chemin Joseph Aiguier, 13402 Marseille Cedex 20. France.

▽ Present address: IDS Intelligent Detection Systems, 152 Cleopatra Dr., Nepean, Ontario K2G 5X2, Canada.

[1] Abbreviations: BChl, bacteriochlorophyll; FT, Fourier transform; LH, light-harvesting; P, primary electron donor; RC, reaction center; *Rb*., *Rhodobacter*; *Rps*., *Rhodopseudomonas*; *Rsp*., *Rhodospirillum*.

10.1021/bi990723z CCC: $18.00
Published on Web 08/04/1999

properties of the BChls of LH proteins has been extensively studied, and the relative importance of these interactions has been experimentally quantified (*8*−*15*). In bacterial RCs, the changes in the redox potential of the P BChls induced by their interactions with neighboring histidines have been characterized (*16*−*18*). The role of the electrostatic properties of the protein binding pocket was studied in the case of the monomer BChl (B800) bound to the LH2 protein, and their influence was experimentally quantified (*14*).

The role played by the surrounding protein in tuning the electronic properties of BChl was first suggested from analysis of the X-ray crystal structure of the soluble antenna protein from *Prosthecochloris aestuarii* (*19, 20*). This protein contains a particularly distorted pigment, the macrocycle of which deviates significantly from planarity, which was proposed to relate to unusual absorption properties, i.e. an absorption maximum located at 820 nm at low temperature (*21*). The influence of conformational distortions has also been shown in model studies with strained porphyrins (*22* and references therein). However, there was no direct experimental evidence of how conformational changes imposed by the surrounding protein tune the electronic properties of BChl in photosynthetic proteins. Recently there has been a dramatic increase in our knowledge of bacterial complexes, resulting from the determination of high-resolution (≥2.7 Å) X-ray crystal structures of the RCs from *Rhodopseudomonas viridis* (*23*) and *Rhodobacter sphaeroides* (*24*) and of the LH2 complexes from *Rhodopseudomonas acidophila* 10050 (*25*) and *Rhodospirillum molischianum* (*26*), and a low-resolution electron crystallographic structure of the LH1 complex from *Rhodospirillum rubrum* (*27*). In the structural models derived from X-ray diffraction patterns of crystals of the RC and LH2 complexes, BChl molecules with distorted macrocycles were clearly identified in the primary electron donor of the RC and in the 850 nm-absorbing BChls of LH2. These distortions pose a number of interesting questions. First, it is not yet clear what role these distortions play in tuning the electronic properties of the particular BChls. Second, very little is known about the BChl conformations in RCs and/or LH2 proteins that have not yet been crystallized, and so we do not know how general these distortions are. Finally, knowledge of more subtle conformational changes of BChls, which is vital to our understanding of their properties, is difficult to determine from electron density maps of protein crystals at the resolutions currently achieved.

Fourier transform (FT) resonance Raman spectroscopy with 1064 nm excitation yields selective conformational information on the BChl *a* molecule(s) responsible for the redmost absorption peak in the various complexes described above (i.e., 850 or 880 nm-absorbing BChl *a* molecules in LH2 and LH1, respectively, and the P BChls in the RC). This technique was recently shown to be capable of measuring distortions of the BChl *a* macrocycle as small as 0.02 Å (*28*), and a systematic analysis of those vibrational modes sensitive to conformational changes was recently performed (*28*). This study showed that the frequencies of six modes in FT-Raman spectra of BChl *a* derivatives were linearly dependent on the core size of the macrocycle, which was defined as the average distance between the pyrrole nitrogens and the projection of the central ion onto the macrocycle plane. For pentacoordinated BChl *a*, the frequencies of these modes, denoted as R_1−R_6, are observed at 1609, 1536, 1445, 1158, 1140, and 1017 cm^{-1}, respectively. In this work, we have used FT resonance Raman spectroscopy to study the conformation of BChl *a* molecules in RC and LH complexes from various purple bacteria, and we discuss our data in the light of available structural data from X-ray crystallographic studies.

MATERIALS AND METHODS

Sample Preparation. Photochemical reaction centers were isolated from carotenoid-containing (strain 2.4.1) and carotenoidless (strain R26.1) strains of *Rb. sphaeroides.* Cells were grown photoheterotrophically at 28 ± 2 °C in glass bottles located between banks of incandescent lamps. Membranes were prepared and the RCs were purified essentially by the method described by ref *29*. In the case of *Rsp. rubrum* strain $G9^+$, the isolation of the carotenoidless RCs were carried out as described previously (*29, 30*). The LH1 antenna of *Rsp. rubrum* was purified from RC-depleted chromatophores of strain $G9^+$, according to the procedures in Sturgis and Robert (*31*).

Rps. acidophila, strain 7750, was grown photoheterotrophically at 28 ± 2 °C in glass bottles located between banks of incandescent lamps at two extreme light intensities. The high-light intensity was in excess of 10 W m^{-2} while the low-light intensity was approximately 0.1 W m^{-2}. Cultures were regularly transferred to ensure a constant low culture optical density. This minimized any self-shading caused by the cells themselves, which would precipitate a low-light regime. This ensured that the final inocula either contained only high- or low-light adapted intracytoplasmic membranes. These membranes contained 850 and 820 nm-absorbing LH2 complexes, respectively. Cells were harvested, membranes were prepared, and proteins were isolated essentially by the method described by ref *32*. The 850 nm-absorbing LH2 complexes from *Rsp. molischianum* were isolated as described previously (*33*).

Spectroscopy. Room-temperature FT Raman spectra were recorded at 4 cm^{-1} resolution by using a Bruker IFS 66 interferometer coupled to a Bruker FRA 106 Raman module equipped with a continuous Nd−YAG laser, as detailed in Mattioli et al. (*34*). All spectra were recorded at room temperature with backscattering geometry from concentrated proteins (final optical density 100 cm^{-1}) held in standard aluminum cups. Spectra were the result of 1000−10 000 coadded interferograms. Spectra of BChl *a* in diethyl ether were recorded as previously described by Näveke et al. (*28*).

RESULTS

Reaction Centers. The FT-Raman spectra of the carotenoidless RCs from *Rsp. rubrum* strain G_9^+ and *Rb. sphaeroides* strain R26.1 and isolated, monomeric BChl *a* in diethyl ether are very similar to one another (Figure 1). The most noticeable difference between them is a variation in the intensity of the 925 cm^{-1} band, which is stronger in the RCs than in isolated pigment. As summarized in Table 1 (columns 1−3), very few significant band shifts were observed when these spectra were compared. The largest difference concerned the band at 1358 cm^{-1} in the spectrum of isolated BChl *a* (Figure 1a), which was downshifted to 1352 cm^{-1} in the RC spectra. Three of the bands that have

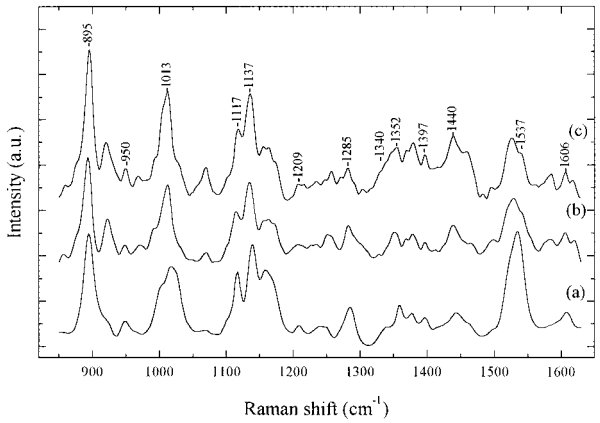

FIGURE 1: FT-Raman spectra (850−1620 cm^{-1} region) of (a) BChl *a* in diethyl ether, (b) reaction centers from *Rb. sphaeroides*, strain R26.1, and (c) reaction centers from *Rsp. rubrum*, strain G_9^+. Spectra were taken at room temperature; excitation wavelength 1064 nm; spectral resolution 4 cm^{-1}.

been shown to exhibit a frequency that is linearly dependent on the BChl macrocycle core size also showed some variations in position. The modes termed R_3, R_5, and R_6, which are observed in the spectrum of BChl *a* in ether at 1445, 1140, and 1017 cm^{-1}, were downshifted in the RC spectra to 1440, 1137, and 1013 cm^{-1}, respectively. It must be emphasized that no significant differences were found between the FT-Raman spectra of the RCs from *Rb. sphaeroides* and *Rsp. rubrum.*

Antenna Complexes. Considerably larger differences were observed in the Raman spectra of LH complexes (Figure 2). In the spectra, which mainly arise from protein-bound BChl *a*, a number of bands were shifted relative to their position in the spectrum of BChl *a* in diethyl ether, most noticeably in the 1340−1415 cm^{-1} region (see Table 1, columns 1, 4, 6, and 7). Different trends were seen among the bands discussed in the introduction that have been shown to be sensitive to the molecular core size of BChl *a*. Both the R_1 (1609 cm^{-1}) and R_3 (1445 cm^{-1}) bands showed the same frequency in the spectra of the antenna complexes as in the spectrum of isolated BChl *a* in diethyl ether. The exceptions are the R_1 band in the spectrum of the LH2 complex from strain 2.4.1, which was downshifted to 1604 cm^{-1}, and the R_3 band in the spectrum of the LH2 antenna of *Rps. molischianum* (Table 1, column 10), which was downshifted to 1441 cm^{-1}. The position of the R_2 band appeared to be constant, varying only between 1536 and 1537 cm^{-1}. It should be noted that the R_2 band is complex and that there are indications of changes in the relative intensities of its individual components. There was a splitting of band R_5 (1140 cm^{-1}) in the spectrum of both types of carotenoidless antennas (Figure 2b,c), which was slightly more pronounced in the carotenoidless LH2 antenna (Figure 2b). Similarly, there was a clear splitting of the R_6 band in the spectrum of the carotenoidless LH1 antenna (Figure 2c), resulting in the appearance of a new 1029 cm^{-1} component that was not seen in either of the spectra of LH2 antenna. The most obvious difference between the spectrum of BChl *a* in diethyl ether and those of antenna-bound BChl *a* is found for the intense R_4 band, which showed a 17 cm^{-1} shift from 1158 cm^{-1} in solvent to 1175 cm^{-1} in the spectra of the LH complexes. This region is expanded in Figure 3 for BChl *a* in ether and the carotenoidless LH1 and LH2 complexes, which includes modes R_4 (1158 cm^{-1}) and R_5 (1140 cm^{-1}). The differences between the spectra were complex, as at least four components contribute to the spectrum in this region. In the spectrum of BChl *a* in ether (Figure 3a), the frequencies of the four components (obtained from spectral deconvolution, data not shown) were at 1117, 1142, 1158, and 1168 cm^{-1}. In the spectra of the LH antennae (Figure 3b,c) four components were also evident, at 1116, 1137, 1142, and 1175 cm^{-1} in the spectrum of LH1 and at 1119, 1132, 1142, and 1175 cm^{-1} in the spectrum of LH2. Assuming similar relative intensities of these components, the 1158 and 1168 cm^{-1} bands present in the spectrum of BChl *a* in diethyl ether seem to shift to 1175 cm^{-1} in the spectra of the antenna complexes. We cannot entirely disregard the possibility that the intensity of the 1158 cm^{-1} band decreases while the 1168 cm^{-1} band upshifts. However, in that case the resulting band at 1175 cm^{-1} should be much less intense than that actually observed in the antennae spectra, unless it were to be accompanied by a dramatic increase in scattering intensity. These shifts in modes R_4 and R_5 suggest that there are significant conformational differences between BChl in the carotenoidless antennae from purple bacteria and BChl in diethyl ether (see Discussion below). The R_5 band occurring at 1142 cm^{-1} in the spectrum of BChl *a* in ether is split in the spectra of protein-bound BChl *a*. In the LH2 complex from *Rb. sphaeroides* strain R26.1, this splitting gives rise to two separate components at 1132 and 1142 cm^{-1}, while in the LH1 complex from *Rps. rubrum* strain G_9^+ the low-frequency component appears only as a shoulder of the 1142 cm^{-1} band. Spectral deconvolution and Gaussian analysis suggest that the actual frequency of this component is 1135 cm^{-1} (data not shown). Therefore, two of the six R_{1-6} bands (R_5 and R_6) are split in the spectra of the antennae complexes. The most obvious explanation for this is that there are two types of BChl molecule responsible for the lowest energy absorption band in the LH complexes and that they have different conformations.

In carotenoid-containing antennae, the FT-Raman contributions arising from these conjugated polyene molecules interfere with the detection of those of BChl *a* (*35*). In the region between 900 and 1550 cm^{-1}, the bands arising from carotenoid vibrational modes mainly contribute at 1150 and 1520 cm^{-1} (denoted by car in Figure 2d and Table 1). Therefore, in the vicinity of these two carotenoid bands the analysis of the frequency of the bands arising from BChl *a* molecules is difficult. However, comparison of the different LH2 proteins from *Rb. sphaeroides*, strains R26.1 and 2.4.1 (Figure 2, spectra b and d, respectively), shows that in regions not affected by the carotenoid contributions at 1150 and 1520 cm^{-1}, most of the frequencies observed were identical in the carotenoidless and carotenoid-containing LH2 complexes, and this appeared to be the case for all of the antennae investigated (Table 1). This indicates that the conformations of the low-energy-absorbing BChl *a* molecules in the carotenoid-containing LH complexes are close to those observed in the carotenoidless antennae. Shown in Figure 4 is the 1080−1220 cm^{-1} region of the FT-Raman spectra of different carotenoid-containing LH1 and LH2 proteins from *Rb. sphaeroides* strain 2.4.1, the 850 and 820 nm-absorbing LH2 complexes from *Rps. acidophila* strain 7050, and the LH2 complex from *Rsp. molischianum*. In all of these spectra a band was present at approximately 1175 cm^{-1} which was

Table 1: Frequencies of the Main Bands of FT-Raman Spectra of BChl *a* in Ether and Various RC and LH Proteins[a]

BChl ether	RC R26.1	RC G_9+	LH1 G_9^+	LH1 2.4.1	LH2 R26.1	LH2 2.4.1	LH2[b] *acid*. I[b]	LH2 *acid*. II	LH2 *mol*.[d]	*e*
1609	1606	1606	1608	1609	1608	1604	1608	1608	1608	R1
1536	1530−1537	1530−1537	1537	car[f]	1532−1537	car	car	car	car	R2
1445	1440	1440	1444	1445	1445	1445	1444	1445	1441	R3
1397	1397	1397	1409	1412	1415	1408				
1377	1379	1379	1385	1385	1388	1386	1387	1396	1385	
1358	1352	1352	1371	1372	1373	1372	1372	1376	1375	
1340	1340	1340	1347	1346	1347	1348	1348			
1285	1285	1285	1285	1285	1285	1284	1286	1285	1288	
1273 (?)	1273	1273	1273	1277	1273	1275	1275			
1209	1209	1209	1212	car	1209	1212	1212	1212	1210	
1158/1168	1159/1170	1159/1170	1175	1174	1175	car	1173	1173	1174	R4
1140	1137	1137	1142/1137	car	1142/1132	car	car	car	car	R5
1117	1115	1117	1116	1116	1119	1117	1118	1117	1118	
1024	1024	1026	1029	car	1024	car	car	car	car	
1017	1013	1013	1017	car	1017	car	car	car	car	R6
1002	1002	1002		car		car	car	car	car	
967	969	968	967	968	967	968	967	968	969	
950	950	950	950	949	950	949	950	950	952	
895	894	895	896	897	895	895	894	897	897	

[a] Observed at Room Temperature, with 1064 nm excitation. All frequencies are given in reciprocal centimeters. [b] *Rps. acidophila* B800−850 complex. [c] *Rps. acidophila* B800−820 complex. [d] *Rsp. molischianum*. [e] Position of the bands sensitive to the molecular core size. [f] Presence of intense carotenoid bands.

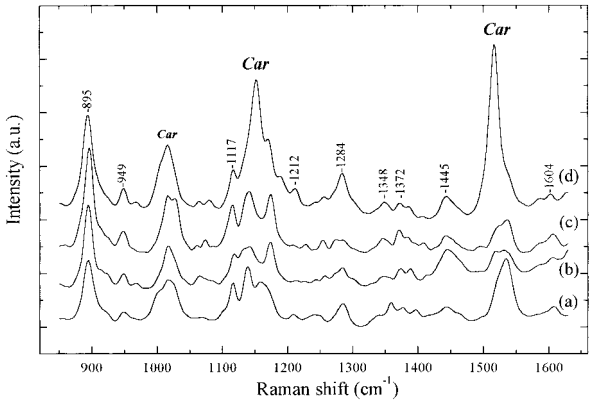

FIGURE 2: FT-Raman spectra (850−1620 cm^{-1} region) of (a) BChl *a* in diethyl ether, (b) LH2 pigment protein complex from *Rb. sphaeroides*, strain R26.1; (c) LH1 pigment protein complex from *Rsp. rubrum*, strain G_9^+; and (d) LH2 pigment protein complex from *Rb. sphaeroides*, strain 2.4.1. Spectra were taken at room temperature; excitation wavelength 1064 nm; spectral resolution 4 cm^{-1}.

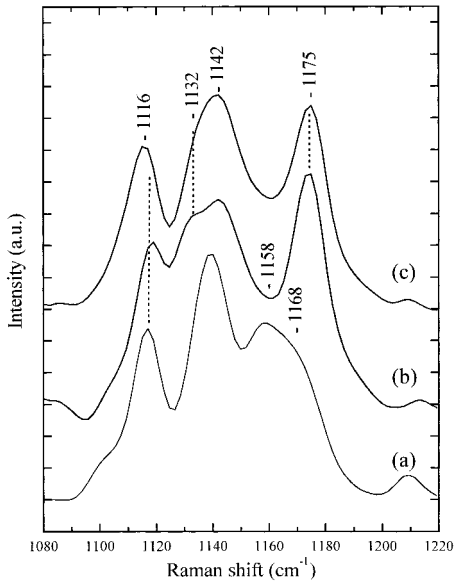

FIGURE 3: FT-Raman spectra (1080−1220 cm^{-1} region) of (a) BChl *a* in diethyl ether; (b) LH2 proteins from *Rb. sphaeroides*, strain R26.1; and (c) LH1 proteins from *Rsp. rubrum*, strain G_9^+. Spectra were taken at room temperature; excitation wavelength 1064 nm; spectral resolution 4 cm^{-1}.

not observed in the FT-Raman spectrum of isolated carotenoid molecules (Figure 4a; see also ref *35*). As Raman spectra of carotenoids are insensitive to their surrounding environment (*36*), it is possible to subtract the spectrum of isolated spheroidenone (Figure 4a) from that of the LH2 complex from *Rb. sphaeroides* (Figure 4b). The difference spectrum obtained (Figure 4g) is nearly identical to the FT-Raman spectra of carotenoidless LH1 and LH2 antennae proteins (Figure 4h). It is thus possible to conclude that the spectral differences observed in this region between BChl *a* in carotenoidless antennae and in BChl *a* in diethyl ether are conserved among all the LH proteins we have studied.

DISCUSSION

When a 1064 nm excitation wavelength is used, FT-Raman spectra of RCs from purple bacteria contain contributions mainly from the two BChls of the primary electron donor (*34*), and those of the LH complexes contain contributions mainly from the BChl *a* molecules responsible for the lowest energy transition (*14*). FT-Raman spectra recorded under these conditions thus yield selective information on the conformational state of these molecules, which are all involved in pigment−pigment interaction. To extract this information, comparisons must be made between spectra of protein-bound BChl *a* and spectra of BChl *a* in a solvent in which the ligand number is similar. Spectra of BChl *a* in diethyl ether were chosen as a reference in this study. It is well established that in this solvent, and under our experimental conditions, isolated BChl *a* molecules are monomeric and their central Mg atom is pentacoordinate (*28*). This Mg coordination state is the same as that most generally observed in RC and LH proteins from purple photosynthetic bacteria (*29*, *37*). As discussed in Lapouge et al. (*38*), as long as the coordination state of the central Mg does not change, FT-

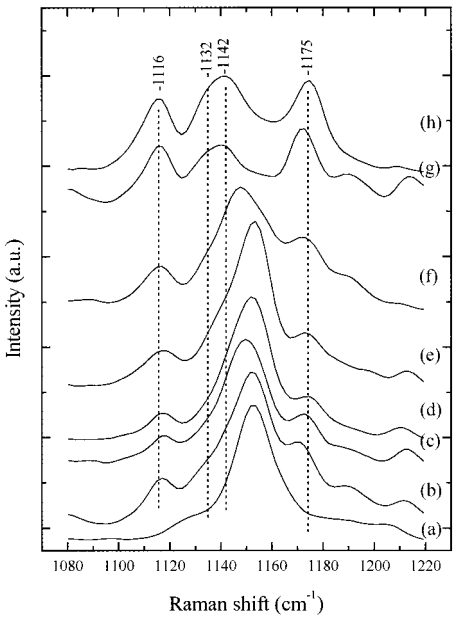

FIGURE 4: FT-Raman spectra (1080−1220 cm^{-1} region) of (a) isolated spheroidenone; (b) LH2 proteins from *Rb. sphaeroides*, strain 2.4.1; (c) LH1 proteins from *Rb. sphaeroides*, strain 2.4.1; (d) 850 nm-absorbing LH2 from *Rps. acidophila*, strain 7750; (e) 820 nm-absorbing LH2 from *Rps. acidophila*, strain 7750; and (f) LH2 from *Rsp. molischianum*, strain DSM 119. (g) Computed difference between spectra b and a. (h) LH1 of the carotenoidless strain G_9^+ of *Rsp. rubrum*, for comparison with spectrum g. Spectra were taken at room temperature; excitation wavelength 1064 nm; spectral resolution 4 cm^{-1}.

Raman spectra of isolated BChl *a* are relatively insensitive to the physicochemical properties of the solvent used, such as the dielectric constant or refractive index. Indeed, only the bands arising from the carbonyl stretching frequencies of the BChl *a* molecules showed shifts greater than 2 cm^{-1} over a wide range of different dielectric constants or refractive indices (*38*). The frequencies of the bands in the 900−1610 cm^{-1} region observed in diethyl ether are thus characteristic of BChl *a* molecules possessing a 5-coordinated central Mg atom, in a relaxed conformational state, as no steric hindrance may impose an energetically unfavorable conformation in a solvent at room temperature.

Bacterial Reaction Centers. From the data presented above it is apparent that the FT-Raman spectra of bacterial RCs are very similar to that of isolated BChl *a* in solvent. In many respects, this suggests that the conformation of both BChl molecules that constitute the primary electron donor is similar to that observed in solvents, i.e., that the proteic binding site does not impose significant strain on the conformation of the macrocycle. However, among the bands sensitive to deformation of the macrocycle, three appear to experience limited downshifts in frequency in the spectra of bacterial RCs; namely, the 1440 (−5 cm^{-1}), 1137 (−3 cm^{-1}), and 1013 cm^{-1} (−4 cm^{-1}) modes. Similar downshifts were observed in vitro when the central Mg atom of BChl *a* was changed from 5- to 6-coordination (*28*). However, these shifts were accompanied by downshifts of the other R_{1-6} modes, the frequencies of which could be linearly correlated with the BChl *a* core size (*28*). In the well-documented case of porphyrins (*39*), it is clear that this linear correlation represents a first-order approximation, and that a much better linear correlation can be found between the Raman band frequencies and the values of the C_aNC_a angles. The specific pattern of band shifts observed thus depends on the type of distortion imposed on the macrocycle. The fact that only three of these modes, R_3, R_5, and R_6, change frequency in the spectra of bacterial RCs indicates that the binding of the BChl to these proteins imposes a different geometry on the molecule than that imposed on metal-substituted bacteriopheophytin molecules in vitro. It is worth noting that none of the bands that are observed to shift in the FT-Raman spectrum of P are (inhomogeneously) broadened. This suggests that most of the distortions we observe should be common to both of the BChls that constitute P.

In most of the model structures that have been derived from X-ray crystallographic studies, it appears that the BChls of P are slightly distorted, and in particular that both conjugated macrocycles are clearly domed (*24*, *40*). According to the FT-Raman results presented above, it is possible to conclude that this conformation should be close to that adopted by BChl *a* in ether. It is worth noting that resonance Raman is sensitive to molecular distortions as small as 0.05 Å and that most of the conformational differences discussed here should result in a root-mean-square (rms) deviation that is much smaller than 0.2 Å. Differences of this order are well below the limits of detection of X-ray crystallography at its current resolution on bacterial reaction centers. To illustrate this, the rms deviation in the position of the backbone α carbon atoms between two independently determined structures for the wild-type *Rb. sphaeroides* RC (*24*, *40*), both at a resolution of approximately 2.6 Å, was on the order of 0.35 Å (*40*).

Antenna Proteins. As mentioned above, FT-Raman spectra of antenna proteins from purple bacteria mainly arise from the BChls responsible for the redmost absorption of these complexes, i.e., the 850 or 820 nm-absorbing BChls in LH2 and the 875 nm-absorbing BChls in LH1. The FT-Raman spectra of LH1 and the different spectral forms of LH2 (the B800−820 and B800−850 nm-absorbing proteins), including the unusual LH2 complex from *Rps. molischianum* (*33*), are all extremely similar. Moreover, and in contrast with our observations on RCs, the frequencies of some of the Raman bands in the spectra of LH complexes exhibit dramatic shifts relative to those observed for BChl *a* in diethyl ether. This is true in particular for all of the bands between 1350 and 1420 cm^{-1} and for the core-size-sensitive bands R_4 and R_5. As for RCs, the fact that only some of the core-size-sensitive bands are shifted in antenna proteins indicates that the constraints experienced by the BChl *a* molecules upon binding to the antenna proteins result in a different geometry of the BChl macrocycle than that observed when the size of the central ion of these molecules is changed. The number and magnitude of the shifts observed in antenna spectra indicate that the conformation of the BChl *a* bound to these proteins is far from relaxed. In particular, the appearance of a single band at 1175 cm^{-1} in these spectra represents a shift of 17 and 7 cm^{-1} relative to the two components observed at 1158 and 1168 cm^{-1} respectively in the spectra of BChl *a* in diethyl ether or in RCs. The high frequency exhibited by these modes is similar to that observed in spectra of Cu−Bpheo (*28*), the core size of which is reduced by as much a 2% relative to 5-coordinated BChl *a* (as a comparison, the distortion of the molecule induced by a change in Mg coordination results in only a 0.6% variation in this value).

It is thus possible to conclude that the BChl *a* molecules in light-harvesting proteins exhibit a significant distortion of their conjugated macrocycle and that this distortion is conserved among the different LH complexes in different bacteria.

Certain bands appeared to be inhomogeneously broadened in the FT-Raman spectra of the LH proteins. The mode at 1142 cm^{-1} clearly split into two components in both the LH1 and LH2 spectra. The magnitude of this splitting was larger for LH2 than for LH1, and two clear components were observed in the spectra of the former complexes, at 1132 and 1142 cm^{-1}, while in the spectra of LH1 the splitting resulted in the presence of two convoluted bands at 1137 and 1142 cm^{-1}. Similarly, the band at 1117 cm^{-1} was clearly split in the spectra of LH1 into two components at 1117 and 1128 cm^{-1}. As these modes are known to be sensitive to the molecular distortion of BChl *a* molecules (*28*), it can be concluded from these splittings that the BChl molecules bound to the light-harvesting protein that contributes to the lowest energy optical transition exist in different conformations. As LH proteins are built up from subunits containing two polypeptides (α and β), each binding one of the BChl *a* molecules involved in the lowest energy transition, it seems reasonable to conclude that the BChl bound to the α polypeptide has a different conformation than that bound to the β polypeptide. In LH2, this difference in conformation results in an approximately 10 cm^{-1} shift of band R_5, while in LH1 it results in a smaller splitting of this band but is accompanied by an additional splitting of the R_1 mode. This constitutes the main indication that the conformation of the BChl in LH1 should be similar, but not identical, to that found in LH2 proteins.

In the model structure derived from X-ray crystallographic studies of the LH2 complex from *Rps. acidophila*, the BChls bound to the α- and β-polypeptides (termed $BChl_\alpha$ and $BChl_\beta$, respectively) indeed exhibit different conformations. However, at the resolution of 2−3 Å, differences in structure on the order of 0.3 Å or less cannot be regarded as being significant. This number can be compared with the distances between opposite pyrrole nitrogens in magnesium tetraphenylporphyrin which are 4.098 and 4.077 Å when the central Mg is five-coordinate and 4.14 Å when it is six-coordinate (*42*); i.e., the change in Mg coordination induces a variation of these distances of less than 0.07 Å. However, although small, this change corresponds to macrocycle distortions that are able to induce a shift of the R_1 mode by as much as 10 cm^{-1}. As a result, BChl structures derived from much higher resolution electron density maps would be required if they are to be any direct help in the interpretation of Raman data. A precise description of the distortions of the BChl a macrocycle, as measured by Raman spectroscopy, requires more extensive studies of model compounds, but it can be estimated by comparing the shift observed in vivo to those associated by the distortion induced in vitro when the Mg central ion is replaced by other smaller metal ions. As stated above, the largest shift observed, which concerns the band at 1175 cm^{-1}, is of the same magnitude of the shift observed when the Mg is replaced by a Cu ion (*37*). In the crystal structure of Cu-tetraphenylporphyrin, it may be observed that presence of the small Cu ion in the center of the porphyrin induces deviations of the pyrrolic carbons out of the average plane of the molecule by as much as 0.25 Å (*43*). Although they constitute an approximate estimate of what may happen in vivo for bacteriochlorophylls, such deviations are likely to represent what should be expected in the structure of LH complexes of purple bacteria.

It would of course be of great interest to evaluate how the distortions of the BChl macrocycle may influence their monomeric absorption properties. Such an influence has been predicted by theoretical calculations (*44*), and it should, in turn, influence the electronic properties of LH1 and LH2. In the particular case of the 800 nm-absorbing BChl of LH2 proteins, it was recently shown that the distortion of the BChl *a* macrocycle should not result in more than 150 cm^{-1} shift of the Q_y of this molecule (*14*). On the other hand, in the Fenna−Matthews−Olson light-harvesting protein from green sulfur bacteria, it is assumed that the particular conformation of one of the bound BChl is responsible for a ca. 240 cm^{-1} shift in its Q_y transition (*45* and references therein). FT-Raman results suggest that the BChl responsible for the red-shifted transition in LH complexes from purple bacteria do not share exactly the same conformation. It is thus likely that their individual absorption properties are slightly different. Recent calculations using as a starting point the conformations of the BChl in LH2 derived from the crystal structure led to quite a significant difference (90 cm^{-1}) between the absorption of the individual monomers (*46*). Similarly, the loss of degeneracy between the individual absorption of these molecules was recently proposed to be responsible for the red shift of the zero crossing of the CD spectra of LH2 relative to their absorption maxima (*47*). However, it is at the moment impossible to confirm experimentally these calculations. Furthermore, many different physical mechanisms may underlie such a loss of degeneracy, e.g., differences in the dielectric properties of the BChl binding sites. Future experiments combining site-selected mutagenesis and FT-Raman measurements will help in creating LH proteins with altered BChl conformations, to precisely determine to what extent pigment conformation is involved in tuning the absorption properties of LH from purple bacteria.

CONCLUSION

FT-Raman spectroscopy provides a very accurate method for studying BChl conformation within photosynthetic proteins from purple bacteria and is able to detect differences in conformation that are well below the limits of detection in current X-ray crystal structures. The shifts observed between the spectrum of isolated BChl and spectra of BChl in light-harvesting proteins and/or RCs lead to the following conclusions: (i) The macrocycles of BChl *a* molecules constituting the primary electron donor in the RC are in a conformation that is close to the relaxed conformation observed for BChl *a* in diethyl ether. (ii) This is not the case for the BChl *a* molecules that are responsible for the long-wavelength absorption transitions in both the LH1 and LH2 antenna complexes. (iii) In the antenna proteins, the conformation of $BChl_\alpha$ and $BChl_\beta$ are noticeably different. The molecular origin of these strained conformations of the antenna-bound BChls, as well as its influence on the antenna absorption, are currently being investigated in our laboratories.

ACKNOWLEDGMENT

We thank Dr. Paul Fyfe and Dr. Mike Jones for helpful discussions.

REFERENCES

1. Moss, D. A., Leonhard, M., Bauscher, M., and Mäntele, W. (1991) *FEBS Lett. 283*, 33−36.
2. Williams, J. C., Alden, R. G., Murchisson, H. A., Peloquin, J. M., Woodbury, N. W., and Allen, J. P. (1992) *Biochemistry 31*, 11029−11037.
3. Nagarajan, V., Parson, W. W., Davis, D., and Schenck, C. C. (1993) *Biochemistry 32*, 12324−12336.
4. Jia, Y., Di Magno, T. J., Chan, L. K., Wang, Z., Du, M., Hanson, D. K., Schiffer, M., Norris, J. R., and Fleming, G. R. (1993) *J. Phys. Chem. 97*, 13180−13191.
5. Beekman, L. M. P., Visschers, R. W., Monshouwer, R., Heer-Dawson, M., Mattioli, T. A., McGlynn, P., Hunter, C. N., Robert, B., and van Stokkum, I. H. M. (1995) *Biochemistry 34*, 14712−14721.
6. Fowler, C. F., Nugent, N. A., and Fuller, R. C. (1971) *Proc. Natl. Acad. Sci. U.S.A. 68*, 2278−2282.
7. Prince, R. C., and Olson, J. M. (1976) *Biochim. Biophys. Acta 423*, 357−362.
8. Fowler, G. J. S., Sockalingum, G. D., Robert, B., and Hunter, C. N. (1994) *Biochem. J. 299*, 695−700.
9. Olsen, J. D., Sockalingum, G. D., Robert, B., and Hunter, C. N. (1994) *Proc. Natl. Acad. Sci. U.S.A. 91*, 7124−7128.
10. Olsen, J. D., Sturgis, J. N., Westerhuis, W. H. J., Fowler, G. J. S., Hunter, C. N., and Robert, B. (1997) *Biochemistry 36*, 12625−12632.
11. Sturgis, J. N., Jirsakova, V., Reiss-Husson, F., Cogdell, R. J., and Robert, B. (1995) *Biochemistry 34*, 517−523.
12. Sturgis, J. N., Hagemann, G., Tadros, M. H., and Robert, B. (1995) *Biochemistry 34*, 10519−10524.
13. Sturgis, J. N., Olsen, J. D., Robert, B., and Hunter, C. N. (1997) *Biochemistry 36*, 2772−2778.
14. Gall, A., Fowler, G. J. S., Hunter, C. N., and Robert, B. (1997) *Biochemistry 36*, 16282−16287.
15. Sturgis, J. N., Gall, A., Ellervee, A., Freiberg, A., and Robert, B. (1998) *Biochemistry 37*, 14875−14880.
16. Mattioli, T. A., Williams, J. A., Allen, J. P., and Robert, B. (1994) *Biochemistry 33*, 1636−1643.
17. Mattioli, T. A., Lin, X., Allen, J. P., and Williams, J. C. (1995) *Biochemistry 34*, 6142−6152.
18. Ivancich, A., Artz, K., Williams, J. C., Allen, J. A., and Mattioli, T. A. (1998) *Biochemistry 37*, 11812−11820.
19. Matthews, B. W., Fenna, R. E., Bolognesi, M. C., Schmid, M. F., and Olson, J. M. (1979) *J. Mol. Biol. 131*, 259−285.
20. Pearlstein, R. M. (1992), *Photosynth. Res. 31*, 213−226.
21. Olson, J. M., Philipson, K. D., and Sauer, K. (1973) *Biochim. Biophys. Acta 292*, 206−217.
22. Senge, M. O. (1992) *J. Photochem. Photobiol. 16*, 3−36.
23. Deisenhofer, J., Epp, O., Sinning, I., and Michel, H. (1995) *J. Mol. Biol. 246*, 429−457.
24. Ermler, U., Fritzsch, G., Buchanan, S. K., and Michel, H. (1994) *Structure 2*, 925−936.
25. McDermott, G., Prince, S. M., Freer, A. A., Hawthornthwaite-Lawless, A. M., Papiz, M. Z., Cogdell, R. J., and Isaacs, N. W. (1995) *Nature 374*, 517−521.
26. Koepke, J., Hu, X., Muenke, C., Schulten, K., and Michel, H. (1996) *Structure 4*, 581−597.
27. Karrasch, S., Bullough, P. A., and Ghosh, R. (1995) *EMBO J. 14*, 631−638.
28. Näveke, A., Lapouge, K., Sturgis, J. N., Hartwich, G., Simonin, I., Scheer, H., and Robert, B. (1997) *J. Raman Spectrosc. 28*, 599−604.
29. Robert, B., and Lutz, M. (1985), *Biochim. Biophys. Acta 807*, 10−23.
30. Boucher, F., van der Rest, M., and Gingras, G. (1977) *Biochim. Biophys. Acta 461*, 339−357.
31. Sturgis, J. N., and Robert, B. (1994) *J. Mol. Biol. 238*, 445−454.
32. Cogdell, R. J., Durant, I., Valentine, J., Lindsay, J. G., and Schmidt, K. (1983) *Biochim. Biophys. Acta 722*, 427−435.
33. Germeroth, L., Lottspeich, F., Robert, B., and Michel, H. (1993) *Biochemistry 32*, 5615−5621.
34. Mattioli, T. A., Hoffman, A., Robert, B., Schrader, B., and Lutz, M. (1991) *Biochemistry 30*, 4648−4654.
35. Mattioli, T. A., Hoffman, A., Sockalingum, G. D., Schrader, B., Robert, B., and Lutz, M. (1993) *Spectrochim. Acta 49A*, 785−799.
36. Ohashi, N., Ko-Chi, N., Kuki, M., Shimamura, T., Cogdell, R. J., and Koyama, Y. (1996) *Biospectroscopy 2*, 59−69.
37. Lutz, M., and Robert, B. (1987) in *Biological applications of Raman spectroscopy* (Spiro, T. G., Ed.) pp 347−411, Wiley-Intersciences, New York.
38. Lapouge, K., Näveke, A., Sturgis, J. N., Hartwich, G., Renaud, D., Simonin, I., Lutz, M., Scheer, H., and Robert, B. (1998) *J. Raman Spectrosc. 29*, 977−981.
39. Spaulding, L. D., Chang, C. C., Yu, N. T., and Felton, R. H. (1975) *J. Am. Chem. Soc. 97*, 2517−2525.
40. McAuley-Hecht, K. E., Fyfe, P. K., Ridge, J. P., Prince, S. M., Hunter, C. N., Isaacs, N. W., Cogdell, R. J., and Jones, M. R. (1998) *Biochemistry 37*, 4740−4750.
41. Cogdell, R. J., Isaacs, N. W., Freer, A. A., Arrelano, J., Howard, T. D., Papiz, M. Z., Hawthornthwaite-Lawless, A. M., and Prince, S. M. (1997) *Prog. Biophys. Mol. Biol. 68*, 1−27.
42. McKee, V., and Rodley, G. A. (1988) *Inorg. Chim. Acta 151*, 233−236.
43. Fleischer, E. B., Miller, C. K., and Webb, L. E. (1964) *J. Am. Chem. Soc. 86*, 2342−2347.
44. Barkigia, K. M., Chantranupong, L., Smith, K. M., and Fajer, J. (1988) *J. Am. Chem. Soc. 110*, 7566−7567.
45. Vulto, S. I. E., Streltsov, A. M., and Aartsma, T. J. (1997) *J. Phys. Chem. B 101*, 4845−4850.
46. Alden, R. G., Johnson, E., Nagarajan, V., Parson, W. W., Law, C. J., and Cogdell, R. G. (1997) *J. Phys. Chem. B 101*, 4667−4680.
47. Koolhaas, M. H. C., van der Zwan, G., Frese, R. N., and van Grondelle, R. (1997) *J. Phys. Chem. B 101*, 7262−7270.

BI990723Z